

NASA-CR-172,309

NASA Contractor Report 172309

NASA-CR-172309
19840011858

**SURFACE CRACKS IN A PLATE OF FINITE WIDTH
UNDER TENSION OR BENDING**

F. Erdogan and H. Boduroglu

**LEHIGH UNIVERSITY
Bethlehem, Pennsylvania 18015**

**Grant NGR 39-007-011
February 1984**

LIBRARY COPY

MAR 16 1984

**LANGLEY RESEARCH CENTER
LIBRARY, NASA
HAMPTON, VIRGINIA**



**National Aeronautics and
Space Administration**

**Langley Research Center
Hampton, Virginia 23665**

SURFACE CRACKS IN A PLATE OF FINITE WIDTH
UNDER EXTENSION OR BENDING*

by

F. Erdogan and H. Boduroglu**
Lehigh University, Bethlehem, PA

ABSTRACT

In this paper the problem of a finite plate containing collinear surface cracks is considered. The problem is solved by using the line spring model with plane elasticity and Reissner's plate theory. The main purpose of the study is to investigate the effect of interaction between two cracks or between cracks and stress-free plate boundaries on the stress intensity factors and to provide extensive numerical results which may be useful in applications. First, some sample results are obtained and are compared with the existing finite element results. Then the problem is solved for a single (internal) crack, two collinear cracks and two corner cracks for wide range of relative dimensions. Particularly in corner cracks the agreement with the finite element solution is surprisingly very good. The results are obtained for semi-elliptic and rectangular crack profiles which may, in practice, correspond to two limiting cases of the actual profile of a subcritically growing surface crack.

1. Introduction

Surface cracks are among the most common flaws in structural components, particularly in welded structures. Under cyclic loading or under static loading in the presence of corrosive environment any surface flaw has the potential of subcritically growing into a surface crack. Analysis of the structure containing such flaws is needed for modeling and prediction of the corresponding crack propagation rate. A review of the subject and a number of articles dealing with the analysis of the surface crack problem in plates may be found in [1]. At this

* This study was supported by the National Science Foundation under the Grant MEA-8209083 and by NASA-Langley under the Grant NGR 39 007 011.

** Department of Civil Engineering, Istanbul Technical University, Istanbul, Turkey.

point the analytical treatment of the problem appears to be intractable. Therefore, the reliable solutions of the problem seem to be based on numerical techniques, most notably on the finite element method (see, for example, [2] for the solution of a wide plate containing a semi-elliptic surface crack). In recent years, however, there has been some renewed interest in the application of the line spring model which was first described in [3] to the analysis of surface crack problems. The method was used in [4] in conjunction with Reissner's plate theory and the stress intensity factors for a semi-elliptic and a rectangular surface crack were calculated for a wide plate under tension or bending. The semi-elliptic crack results described in [4] compare very favorably with the finite element solution given in [2].

In this paper the general problem is considered for a plate having a finite width. Analytically, it is known that if the stress fields of more than one crack or that of a crack and a stress-free boundary of the plate interact, there would be some magnification in the stress intensity factors. The problem may therefore be important in plate structures having more than one initial surface flaw or having a flaw near or at the boundary. Extensive finite element results for a single central or corner surface crack in a plate of finite width are given in [5] and [6]. Empirically developed expressions for stress intensity factors based on the results given in [5] are also described in [7]. The present study was undertaken partly to show that the line spring model may be used for cracks in finite plates, particularly for corner cracks just as effectively as the infinite plate and partly to supplement the results given in [5] and [6] by, for example, considering the cases of a rectangular crack profile and collinear surface cracks.

2. The General Formulation of the Problem

The problem under consideration is described in Fig. 1. It is assumed that x_1x_3 and x_2x_3 planes are planes of symmetry with respect to loading and geometry and the length of the plate in x_2 direction is relatively long compared to the width $2b$ so that in formulating the

perturbation problem one may assume the plate to be infinitely long. Even though the numerical results are given for uniform tension in x_2 direction and cylindrical bending in x_2x_3 plane applied to the plate away from the crack region, as will be seen from the formulation of the problem, there is no restriction on the external loads provided in the absence of any cracks the membrane and bending resultants in x_1x_3 plane can be obtained for the given plate geometry and the applied loads.

The problem is formulated for the collinear cracks shown in Fig. 1. The single central crack and the edge or the corner cracks are then considered as the special cases. One of the advantages of the line spring model is that the crack profile (as described by the function $L(x_1)$ giving the crack depth) can be arbitrary. However, the actual crack morphology studies indicate that for a given length $2a$ and a depth L_0 the crack profile may be bounded by a semi-ellipse and a rectangle. Hence, in this paper the calculated results will be given only for these two limiting crack shapes.

Ordinarily, the problems of in-plane loading (as expressed as a generalized plane stress problem) and bending of a plate are uncoupled. Consequently, the corresponding through crack problems can be solved independently. For the plate geometry shown in Fig. 1 the plane elasticity and plate bending solutions are given in [8] and [9], respectively. In the case of surface cracks, because of the absence of symmetry in thickness direction, the membrane and bending problems are clearly coupled. As in [9] in this paper, too, a transverse shear theory is used to formulate the bending component of the problem. The particular theory used is that of Reissner's [10] which is a sixth order theory and accounts for all three boundary conditions on the crack surfaces separately.

Referring to Appendix A for normalized quantities and, for example, to [11] for the general formulation, the basic equations of the plate problem may be expressed as follows:

$$\nabla^4 \phi = 0 , \quad (1)$$

$$\nabla^4 w = 0 , \quad (2)$$

$$\kappa \nabla^2 \psi - \psi - w = 0, \quad (3)$$

$$\kappa \frac{1-\nu}{2} \nabla^2 \Omega - \Omega = 0, \quad (4)$$

$$\sigma_{xx} = \frac{\partial^2}{\partial y^2} (h\phi), \quad \sigma_{yy} = \frac{\partial^2}{\partial x^2} (h\phi), \quad \sigma_{xy} = -\frac{\partial^2}{\partial x \partial y} (h\phi) \quad (5)$$

$$\beta_x = \frac{\partial \psi}{\partial x} + \frac{1-\nu}{2} \kappa \frac{\partial \Omega}{\partial y}, \quad \beta_y = \frac{\partial \psi}{\partial y} - \frac{1-\nu}{2} \kappa \frac{\partial \Omega}{\partial x}, \quad (6)$$

$$M_{xx} = \frac{a}{h\lambda^4} \left[\frac{\partial^2 \psi}{\partial x^2} + \nu \frac{\partial^2 \psi}{\partial y^2} + \frac{\kappa}{2} (1-\nu)^2 \frac{\partial^2 \Omega}{\partial x \partial y} \right], \quad (7)$$

$$M_{yy} = \frac{a}{h\lambda^4} \left[\frac{\partial^2 \psi}{\partial y^2} + \nu \frac{\partial^2 \psi}{\partial x^2} - \frac{\kappa}{2} (1-\nu)^2 \frac{\partial^2 \Omega}{\partial x \partial y} \right], \quad (8)$$

$$M_{xy} = \frac{a(1-\nu)}{2h\lambda^4} \left[2 \frac{\partial^2 \psi}{\partial x \partial y} + \frac{\kappa}{2} (1-\nu) \left(\frac{\partial^2 \Omega}{\partial y^2} - \frac{\partial^2 \Omega}{\partial x^2} \right) \right], \quad (9)$$

$$V_x = \frac{\partial w}{\partial x} + \frac{\kappa}{2} (1-\nu) \frac{\partial \Omega}{\partial y} + \frac{\partial \psi}{\partial x}, \quad (10)$$

$$V_y = \frac{\partial w}{\partial y} - \frac{\kappa}{2} (1-\nu) \frac{\partial \Omega}{\partial x} + \frac{\partial \psi}{\partial y} \quad (11)$$

where, in the usual notation, F (or ϕ) is the Airy stress function, N_{ij} , M_{ij} , and V_i , ($i, j=1, 2$) are the membrane, bending, and transverse shear resultants, β_1 and β_2 are the components of the rotation vector, u_1 , u_2 and u_3 are the components of the displacement vector, a^* is a length parameter representing the crack size ($a^*=a$ for $0 < c < d \leq b$ and $a^*=d$ for $c=0$, $d < b$, Fig. 1), E and ν are the elastic constants, the constants κ and λ are defined in Appendix A, ψ and Ω are auxiliary functions defined in [11], and the dimensions h , a , b , c , and d are shown in Fig. 1.

Because of symmetry, it is sufficient to consider the problem for $0 \leq x_1 < b$, $0 \leq x_2 < \infty$ only. Thus, the membrane and bending problems of the plate must be solved under the following boundary and symmetry conditions stated in terms of the normalized quantities (Fig. 1 and Appendix A):

$$u(0, y) = 0, \quad N_{xy}(0, y) = 0, \quad 0 \leq y < \infty, \quad (12)$$

$$N_{xx}(b', y) = 0, \quad N_{xy}(b', y) = 0, \quad 0 \leq y < \infty, \quad (13)$$

$$N_{xy}(x,0) = 0, \quad 0 \leq x < b', \quad (14)$$

$$N_{yy}(x,0) = \frac{1}{E} [-\sigma_{\infty}(x) + \sigma(x)], \quad c' < x < d', \quad (15a)$$

$$v(x,0) = 0, \quad 0 \leq x < c', \quad d' < x < b'; \quad (15b)$$

$$\beta_x(0,y) = 0, \quad M_{xy}(0,y) = 0, \quad v_x(0,y) = 0, \quad 0 \leq y < \infty, \quad (16)$$

$$M_{xx}(b',y) = 0, \quad M_{xy}(b',y) = 0, \quad v_x(b',y) = 0, \quad 0 \leq y < \infty, \quad (17)$$

$$M_{xy}(x,0) = 0, \quad v_y(x,0) = 0, \quad 0 \leq x < b', \quad (18)$$

$$M_{yy}(x,0) = \frac{1}{6E} [-m_{\infty}(x) + m(x)], \quad c' < x < d', \quad (19a)$$

$$\beta_y(x,0) = 0, \quad 0 \leq x < c', \quad d' < x < b'. \quad (19b)$$

The conditions stated above refer to the perturbation problem in which the crack surface tractions are the only nonzero external loads. Consequently, in addition to (12)-(19) it is required that

$$N_{yy}(x,\infty) = 0, \quad N_{xy}(x,\infty) = 0, \quad 0 \leq x < b', \quad (20)$$

$$M_{yy}(x,\infty) = 0, \quad M_{xy}(x,\infty) = 0, \quad v_y(x,\infty) = 0, \quad 0 \leq x < b'. \quad (21)$$

The input functions σ_{∞} and m_{∞} which appear in (15a) and (19a) are defined by

$$\sigma_{\infty}(x) = N_{22}^{\infty}(x_1,0)/h, \quad m_{\infty}(x) = 6M_{22}^{\infty}(x_1,0)/h^2 \quad (22)$$

where $N_{ij}^{\infty}(x_1, x_2)$ and $M_{ij}^{\infty}(x_1, x_2)$, $(i,j=1,2)$ are the membrane and moment resultants in the plate under the actual applied loads in the absence of any cracks. The functions $\sigma(x)$ and $m(x)$ are unknown and are defined

$$\text{by} \quad \sigma(x) = \frac{N(x_1)}{h} = \frac{N(a^*x)}{h}, \quad m(x) = \frac{6M(x_1)}{h^2} = \frac{6M(a^*x)}{h^2} \quad (23)$$

where the membrane load $N(x_1)$ and the bending moment $M(x_1)$ represent the stress component $\sigma_{22}(x_1, 0, x_3)$ in the net ligament $c < x_1 < d$, $-\frac{h}{2} < x_3 < \frac{h}{2} = L$.

In the bending problem the solution of the differential equations (2)-(4) satisfying the symmetry conditions (16) and the regularity conditions (21) may be expressed as follows [9]:

$$w(x,y) = \frac{2}{\pi} \int_0^{\infty} (A_1 + \gamma A_2) e^{-\alpha y} \cos \alpha x \, d\alpha + \frac{2}{\pi} \int_0^{\infty} (C_1 \cosh \beta x + C_2 x \sinh \beta x) \cos \beta y \, d\beta, \quad (24)$$

$$\Omega(x,y) = \frac{2}{\pi} \int_0^{\infty} B_1 e^{-r_1 y} \sin \alpha x \, d\alpha + \frac{2}{\pi} \int_0^{\infty} B_2 \sinh r_2 x \sin \beta y \, d\beta, \quad (25)$$

$$\psi(x,y) = \frac{2}{\pi} \int_0^{\infty} [-A_1 + (2\kappa\alpha - \gamma)A_2] e^{-\alpha y} \cos \alpha x \, d\alpha + \frac{2}{\pi} \int_0^{\infty} [-(C_1 + 2\kappa\beta C_2) \cosh \beta x - C_2 x \sinh \beta x] \cos \beta y \, d\beta, \quad (26)$$

where $A_i(\alpha)$, $B_i(\alpha)$ and $C_i(\beta)$, ($i=1,2$) are unknown functions and

$$r_1 = \left[\alpha^2 + \frac{2}{\kappa(1-\nu)} \right]^{\frac{1}{2}}, \quad r_2 = \left[\beta^2 + \frac{2}{\kappa(1-\nu)} \right]^{\frac{1}{2}}. \quad (27)$$

By substituting from (24)-(26) into (7), (9)-(11) and by using five homogeneous conditions (17) and (18) five of the six unknown functions may be eliminated. The mixed boundary condition (19) would then determine the sixth.

Similarly from the plane stress solution of the plate satisfying the conditions (12), (14) and (20) the stresses and the y -component of the displacement may be expressed as [8]

$$N_{xx}(x,y) = -\frac{2}{\pi} \int_0^{\infty} h_1(\alpha) (1-\alpha y) e^{-\alpha y} \cos \alpha x \, d\alpha - \frac{2}{\pi} \int_0^{\infty} [h_2(\beta) \cosh \beta x + \beta x h_3(\beta) \sinh \beta x] \cos \beta y \, d\beta, \quad (28)$$

$$N_{yy}(x,y) = -\frac{2}{\pi} \int_0^{\infty} h_1(\alpha)(1+\alpha y)e^{-\alpha y} \cos \alpha x \, d\alpha \\ + \frac{2}{\pi} \int_0^{\infty} [(h_2+2h_3) \cosh \beta x + \beta x h_3 \sinh \beta x] \cos \beta y \, d\beta, \quad (29)$$

$$N_{xy}(x,y) = -\frac{2}{\pi} \int_0^{\infty} \alpha y h_1(\alpha) e^{-\alpha y} \sin \alpha x \, d\alpha \\ + \frac{2}{\pi} \int_0^{\infty} [(h_2+h_3) \sinh \beta x + \beta x h_3 \cosh \beta x] \sin \beta y \, d\beta, \quad (30)$$

$$\frac{E}{1+\nu} v(x,y) = \frac{2}{\pi} \int_0^{\infty} \frac{h_1}{\alpha} \left(\frac{1+\kappa}{2} + \alpha y \right) e^{-\alpha y} \cos \alpha x \, d\alpha \\ + \frac{2}{\pi} \int_0^{\infty} \left[\left(\frac{h_2}{\beta} + \frac{1+\kappa}{2} h_3 \right) \cosh \beta x + x h_3 \sinh \beta x \right] \sin \beta y \, d\beta. \quad (31)$$

In this case the unknown functions h_1 , h_2 and h_3 are determined from the remaining boundary conditions (13) and (15).

3. The Integral Equations

If we now replace the mixed boundary conditions (15) and (19) respectively by

$$\frac{\partial}{\partial x} v(x,0) = g_1(x), \quad 0 \leq x < b, \quad (32)$$

$$\frac{\partial}{\partial x} \beta_y(x,0) = g_2(x), \quad 0 \leq x < b, \quad (33)$$

it is seen that by using (17), (18), (13), (32) and (33) all nine unknown functions A_i , B_i , C_i , ($i=1,2$) and h_j , ($j=1,2,3$) which appear in the formulation of the problem given in the previous section may be expressed in terms of the new unknown functions g_1 and g_2 . From the definitions (32) and (33) it also follows that conditions (15b) and (19b) are equivalent to

$$g_i(x) = 0, \quad 0 \leq x < c', \quad d' < x < b', \quad (i=1,2), \quad (34)$$

$$\int_{c'}^{d'} g_i(x) dx = 0, \quad (i=1,2). \quad (35)$$

The functions g_1 and g_2 may now be determined from the two remaining conditions (15a) and (19a). Referring to [8] and [9] for details, the following integral equations may be obtained from these two conditions:

$$\frac{\sigma(x)}{E} - \frac{1}{2\pi} \int_{c'}^{d'} \left[\frac{1}{t-x} + \frac{1}{t+x} + k_1(x,t) - k_1(x,-t) \right] g_1(t) dt = \frac{\sigma_\infty(x)}{E}, \quad (36)$$

$$\begin{aligned} \frac{m(x)}{6E} - \frac{a^*(1-\nu^2)}{2\pi h \lambda^4} \int_{c'}^{d'} \left\{ \left[\frac{3+\nu}{1+\nu} \left(\frac{1}{t-x} + \frac{1}{t+x} \right) - \frac{4\kappa(1-\nu)}{1+\nu} \left[\frac{1}{(t-x)^3} + \frac{1}{(t+x)^3} \right] \right. \right. \\ \left. \left. + \frac{4}{1+\nu} \left[\frac{1}{t-x} K_2(\gamma|t-x|) + \frac{1}{t+x} K_2(\gamma|t+x|) \right] + k_2(x,t) \right. \right. \\ \left. \left. - k_2(x,-t) \right\} g_2(t) dt = \frac{m_\infty(x)}{6E}, \quad c' < x < d', \quad (37) \end{aligned}$$

where K_2 is the modified Bessel function of the second kind, the Fredholm kernels $k_1(x,t)$ and $k_2(x,t)$ are given in Appendix B and the constant γ is given by

$$\gamma = \frac{h}{12(1-\nu^2)a^*}. \quad (38)$$

The functions $\sigma(x)$ and $m(x)$ which appear in (36) and (37) are defined by (23) and represent the membrane and moment resultants of the tensile stress σ_{22} in the net ligament $c' < x < d'$. By using the plane strain solution for an edge crack occupying $(h/2) - L < x_3 \leq h/2$ in a strip of thickness h (Fig. 1) under membrane load $N(x_1)$ and bending moment $M(x_1)$ (applied in x_2x_3 plane) and by expressing the rate of change of the potential energy in terms of crack closure energy and the change of compliance, $\sigma(x)$ and $m(x)$ may be expressed in terms of the crack opening

displacement $2v(x,0,0)$ and the crack opening angle $2\beta_y(x,0)$ as follows (see [1] and [4] for details):

$$\sigma(x) = E [\gamma_{tt}(x)v(x) + \gamma_{tb}(x)\beta_y(x)] , \quad (39)$$

$$m(x) = 6E [\gamma_{bt}(x)v(x) + \gamma_{bb}(x)\beta_y(x)] , \quad (40)$$

where the functions γ_{ij} , ($i,j=t,b$) depend on the local crack depth $L(x)$ and hence are implicit functions of x . The algebraic expressions of these functions are given in [4]. From (32), (33) and (34) by observing that

$$v(x,+0) = \int_{c'}^x g_1(t)dt , \quad \beta_y(x,+0) = \int_{c'}^x g_2(t)dt , \quad (41)$$

and by using (39) and (40), the integral equations (36) and (37) may then be expressed as

$$\begin{aligned} \gamma_{tt}(x) \int_{c'}^x g_1(t)dt - \frac{1}{2\pi} \int_{c'}^{d'} \left[\frac{1}{t-x} + \frac{1}{t+x} + k_1(x,t) - k_1(x,-t) \right] g_1(t)dt \\ + \gamma_{tb}(x) \int_{c'}^x g_2(t)dt = \frac{1}{E} \sigma_\infty(x) , \quad c' < x < d' , \end{aligned} \quad (42)$$

$$\begin{aligned} \gamma_{bt}(x) \int_{c'}^x g_1(t)dt + \gamma_{bb}(x) \int_{c'}^x g_2(t)dt - \frac{a^*(1-\nu^2)}{2\pi h \lambda^4} \int_{c'}^{d'} \left\{ \frac{3+\nu}{1+\nu} \left(\frac{1}{t-x} \right. \right. \\ \left. \left. + \frac{1}{t+x} \right) - \frac{4\kappa(1-\nu)}{1+\nu} \left[\frac{1}{(t-x)^3} + \frac{1}{(t+x)^3} \right] + \frac{4}{1+\nu} \left[\frac{1}{t-x} K_2(\gamma|t-x|) \right. \right. \\ \left. \left. + \frac{1}{t+x} K_2(\gamma|t+x|) \right] + k_2(x,t) - k_2(x,-t) \right\} g_2(t)dt \\ = \frac{1}{6E} m_\infty(x) , \quad c' < x < d' . \end{aligned} \quad (43)$$

From the following asymptotic behavior of the Bessel function $K_2(z)$ for small values of z

$$K_2(z) = \frac{2}{z^2} - \frac{1}{2} + O(z^2 \log z) \quad (44)$$

it can be shown that, as in (42), the integral equation (43) has a simple Cauchy type singular kernel. We also note that the system of singular integral equations (42) and (43) must be solved under the additional conditions (35).

After solving the integral equations (42) and (43) for g_1 and g_2 the Mode I stress intensity factor K at the leading edge of the crack may be obtained by substituting from (39)-(41) into the following expression giving K in a strip containing an edge crack of depth L and subjected to the membrane load σ and bending moment m [4]:

$$K(x) = \sqrt{h} [\sigma(x)g_t + m(x)g_b] \quad (45)$$

where g_t and g_b are functions of L/h and are obtained from the corresponding plane strain solution. From the results given in [12] the expressions for g_t and g_b valid in $0 < L/h \leq 0.8$ may be obtained as follows:

$$g_t(s) = \sqrt{\pi s} (1.1216 + 6.5200s^2 - 12.3877s^4 + 89.0554s^6 - 188.6080s^8 + 207.3870s^{10} - 32.0524s^{12}), \quad (46a)$$

$$g_b(s) = \sqrt{\pi s} (1.1202 - 1.8872s + 18.0143s^2 - 87.3851s^3 + 241.9124s^4 - 319.9402s^5 + 168.0105s^6), \quad (46b)$$

where $s = L(x)/h$.

We now note that for $0 < c' < d' < b$ the solution of the system of singular integral equations is of the form

$$g_i(x) = \frac{G_i(x)}{(x-c')^{\frac{1}{2}}(d'-x)^{\frac{1}{2}}}, \quad c' < x < d', \quad (i=1,2), \quad (47)$$

where the bounded unknown functions G_1 and G_2 may easily be obtained by using the technique described, for example, in [13].

The general crack geometry shown in Fig. 1 has two special cases. The first is the case of a symmetrically located single crack along $-d' < x < d'$, (i.e., $c'=0$, $d' < b'$). In this problem by using the symmetry considerations and by observing that $g_i(t) = -g_i(-t)$, ($i=1,2$), the integral equations (42) and (43) may be somewhat simplified as follows:

$$\begin{aligned} \gamma_{tt}(x) \int_{-d'}^x g_1(t) dt - \frac{1}{2\pi} \int_{-d'}^{d'} \left[\frac{1}{t-x} + k_1(x,t) \right] g_1(t) dt \\ + \gamma_{tb}(x) \int_{-d'}^x g_2(t) dt = \frac{1}{E} \sigma_{\infty}(x), \quad -d' < x < d', \end{aligned} \quad (48)$$

$$\begin{aligned} \gamma_{bt}(x) \int_{-d'}^x g_1(t) dt + \gamma_{bb}(x) \int_{-d'}^x g_2(t) dt - \frac{d(1-\nu^2)}{2\pi h \lambda^4} \int_{-d'}^{d'} \left[\frac{3+\nu}{1+\nu} \frac{1}{t-x} \right. \\ \left. - \frac{4\kappa(1-\nu)}{1+\nu} \frac{1}{(t-x)^3} + \frac{4}{1+\nu} \frac{1}{t-x} K_2(\gamma|t-x|) + k_2(x,t) \right] g_2(t) dt \\ = \frac{1}{6E} m_{\infty}(x), \quad -d' < x < d'. \end{aligned} \quad (49)$$

By using (44) it may again be shown that (49) has a simple Cauchy kernel and the solution of the integral equations is of the following form:

$$g_i(x) = \frac{F_i(x)}{(d'^2 - x^2)^{\frac{1}{2}}}, \quad -d' < x < d', \quad (i=1,2). \quad (50)$$

The second special case is that of corner cracks for which $0 < c' < d' = b'$. In this case it may be shown that as x and t approach the end point b' simultaneously, the kernels k_1 and k_2 in (42) and (43) become unbounded. As shown in [8] and [9] the singular part of these kernels may be separated and may be shown to be

$$k_{1s}(x,t) = k_{2s}(x,t) = \frac{1}{2b'-x-t} - \frac{6(b'-x)}{(2b'-x-t)^2} + \frac{4(b'-x)^2}{(2b'-x-t)^3}, \quad (51)$$

where

$$k_i(x,t) = k_{is}(x,t) + k_{if}(x,t) , (i=1,2) \quad (52)$$

and k_{1f} and k_{2f} are bounded. Together with the Cauchy kernel $1/(t-x)$ in (42) and (43), (51) constitutes a generalized Cauchy kernel. It may be observed that the generalized Cauchy kernel $k_g(x,t) = 1/(t-x) + k_{is}(x,t)$ has the property that $k_g(x,b') = 0$, $k_g(b',t) = 0$ and consequently $g_1(t)$ and $g_2(t)$ are nonsingular at $t=b'$ [8]. Also, in this case the single-valuedness conditions (35) are not valid and, as pointed out in [8], are not needed for a unique solution of the integral equations.

4. The Results

First, some sample problems are solved in order to compare the results obtained from the line spring model in this paper with that obtained from the finite element solutions given in [5] and [6]. In [5] the single symmetric semi-elliptic surface crack problem is considered for a finite plate under uniform tension or cylindrical bending (i.e., $c=0$, $d < b$, Fig. 1). It is assumed that the half length of the plate is $\ell=5d$. Figures 2 and 3 show the comparison of the normalized stress intensity factors calculated along the crack front by the two methods. The normalizing stress intensity factor K_N shown in these figures is defined by

$$K_N = \sigma_\infty \sqrt{\pi L_0} / E(k) , \quad k = \sqrt{1 - L_0^2/d^2} \quad (53)$$

and is the stress intensity factor at the location $x_1 = 0$, $x_2 = 0$, $x_3 = L_0$, (i.e., the end points of the minor axis) of a flat elliptic crack (with semi axes d and L_0) in an infinite solid subjected to uniform tension $\sigma_{22} = \sigma_\infty$ in x_2 direction ($c=0$, Fig. 1). Note that, considering the simplicity of the line spring model, the agreement is not bad. One may also note that at the intersection point of the crack and the plate surface $x = x_1/d = 1$ the results based on the line spring model would not be expected to be very good. Furthermore, at the singular point on the free surface the power of the stress singularity seems to be less

than $1/2$ [14]. Hence, theoretically the stress intensity factor defined on the basis of conventional $1/2$ power should tend to zero as the point on the crack front approaches the free surface at an angle of $\pi/2$. Thus, strictly speaking, the bounded nonzero stress intensity factor given by the finite element solution at the surface do not seem to be correct either.

Figures 4 and 5 show the comparison of the stress intensity factors for a corner crack having the profile of a quarter ellipse and obtained from the line spring model and the finite element solution given in [6]. It should be noted that the finite element results are obtained for a finite plate in which the half length is equal to the total width of the plate and the crack is only on one corner (see the insert in Fig. 4). However, since the crack length-to plate width ratio in both cases is relatively small ($2a/2b = 1/10$ in line spring and $2a/b = 1/5$ in finite element solution), the stress intensity factors for the two geometries should be approximately equal. The figures again show that the agreement is quite good.

The calculated stress intensity factors are given in Tables 1-11. All stress intensity factors were calculated as a function of $x = x_1/a^*$, ($a^*=d$ for a single crack, $a^*=a$ for two cracks, Fig. 1) defining the location along the crack front and of the relative dimensions of the crack and the plate. The following notation and normalizing stress intensity factors are used in presenting the results:

$$\sigma_{b22}(r,0,x_1) \approx \frac{K_b(x)}{\sqrt{2\pi r}}, \quad x = x_1/a^*, \quad (54)$$

$$\sigma_{t22}(r,0,x_1) \approx \frac{K_t(x)}{\sqrt{2\pi r}}, \quad x = x_1/a^* \quad (55)$$

where subscripts b and t correspond to plates under bending and tension, respectively, σ_{22} is the cleavage stress around the crack front, r and θ are the usual polar coordinates at the crack front in x_2x_3 plane (Fig. 1) and K_b and K_t are the corresponding Mode I stress intensity factors. The results are given for uniform membrane load $N_{22} = N_\infty$ and cylindrical

bending moment $M_{22} = M_{\infty}$ away from the crack region. The normalized stress intensity factors shown in the tables are defined by

$$k_b(x) = \frac{K_b(x)}{K_{bo}}, \quad k_t(x) = \frac{K_t(x)}{K_{to}}, \quad (56)$$

$$K_{to} = \left(\frac{N_{\infty}}{h}\right) \sqrt{h} \quad g_t(s_o), \quad s_o = L_o/h, \quad (57)$$

$$K_{bo} = \left(\frac{6M_{\infty}}{h^2}\right) \sqrt{h} \quad g_b(s_o), \quad s_o = L_o/h \quad (58)$$

where L_o is the maximum crack depth and the functions g_t and g_b are given by (45) and (46). One may note that $g_t(s_o)$ and $g_b(s_o)$ are the shape factors obtained from the corresponding plane strain solution of a plate with an edge crack of depth L_o and, for the values of L_o/h shown in the tables, are given by [12] .

$s_o = L_o/h$	0.2	0.4	0.6	0.8
$g_t(s_o)/\sqrt{\pi s_o}$	1.3674	2.1119	4.035	11.988
$g_b(s_o)/\sqrt{\pi s_o}$	1.0554	1.2610	1.915	4.591

Table 1 shows the normalized stress intensity factors at the deepest penetration point of a centrally located single semielliptic surface crack (i.e., $c=0$, $d<b$, Fig. 1) in a plate under uniform tension N_{∞} or bending M_{∞} . Here the crack profile is given by

$$\frac{L^2}{L_o^2} + \frac{x_1^2}{d^2} = 1 \quad (59)$$

or

$$L(x) = L_o \sqrt{1-x^2}, \quad (x = x_1/a^*, \quad a^* = d) \quad (60)$$

and hence $x=0$ is the deepest point on the crack front. This is also the point where k_t assumes its maximum value. For $b/h = 10$ relatively complete and for other plate dimensions some sample results showing the variation of the stress intensity factors along the crack front are shown in Tables 2 and 3. Similar results are shown in Tables 4 and 5 for a single surface crack with a rectangular profile (i.e., for $L(x) = L_0$, $-1 < x < 1$). One may observe that, as expected, generally the stress intensity factors for the rectangular crack are higher than that for the semi-elliptic crack.

The results for two collinear semi-elliptic surface cracks (Fig. 1) are shown in tables 6 and 7. Here the crack profile is defined by (Fig. 1)

$$L(\bar{x}) = L_0 \sqrt{1-\bar{x}^2}, \quad \bar{x} = \frac{x_1 - (c+a)}{a}, \quad -1 < \bar{x} < 1. \quad (61)$$

Table 6 shows the value $k_i(x^*)$, ($i=b,t$) and the location $\bar{x} = x^*$ of the maximum stress intensity factor for various crack geometries in a plate for which $b = 10h$ and $a = h$. The factor $D = a/(a+c)$ determines the crack location. Table 7 shows some sample results giving the distribution of the stress intensity factors along the crack front for two extreme crack locations considered. The skewness in this distribution does not seem to be very significant.

The results for a plate containing two corner cracks having a profile of a quarter ellipse are shown in Tables 8 and 9 (Fig. 1). In this case the crack profile (or the crack depth) L is defined by

$$L(\bar{x}) = L_0 \sqrt{1 - \left(\frac{1-\bar{x}}{2}\right)^2}, \quad \bar{x} = \frac{x_1 - (c+a)}{a}, \quad -1 < \bar{x} < 1. \quad (62)$$

Table 8 shows the normalized Mode I stress intensity factors at the maximum penetration point of the crack which is on the plate boundary $x = b'$ (i.e., for $x_1 = b$ or $\bar{x} = 1$ or $L = L_0$). Some results showing the distribution of the stress intensity factors are given in Table 9. The results were similar for all crack geometries in that for plates under

tension and for those having shallow cracks under bending the maximum stress intensity factor was on the boundary $x = b'$, whereas for deep cracks in plates under bending K was maximum at the surface $x_1 = c$ or $x = c'$ (Fig. 1). For corner cracks with a rectangular profile results similar to those shown in Tables 8 and 9 are given in Tables 10 and 11. For this crack geometry too one may note that generally the stress intensity factors for rectangular cracks are higher than those for the elliptic cracks.

From the formulation of the problem it may be seen that all results in the surface crack problem are dependent on the Poisson's ratio ν of the plate. The stress intensity factors given in this paper are calculated for $\nu = 0.3$. However, as shown [9], since the stress intensity factors are not very sensitive to the Poisson's ratio, the results given in Tables 1-11 should be valid for nearly all structural materials.

References

1. The Surface Crack: Physical Problems and Computational Solutions, J.L. Swedlow, ed. ASME, New York, 1972.
2. I.S. Raju and J.C. Newman, "Stress Intensity Factors for a Wide Range of Semi-Elliptical Surface Cracks in Finite Thickness Plates", *Journal of Engineering Fracture Mechanics*, Vol. 11, pp. 817-829, 1979.
3. J.R. Rice and N. Levy, "The Part-Through Surface Crack in an Elastic Plate", *J. Applied Mechanics*, Vol. 39, pp. 185-194, Trans. ASME, 1972.
4. F. Delale and F. Erdogan, "Line Spring Model for Surface Cracks in a Reissner Plate", *Int. J. Engng. Science*, Vol. 19, pp. 1331-1340, 1981.
5. J.C. Newman, Jr. and I.S. Raju, *Analysis of Surface Cracks in Finite Plates Under Tension or Bending Loads*, NASA Technical Paper 1578, 1979.

6. J.C. Newman, Jr. and I.S. Raju, "Stress Intensity Factor Equations for Cracks in Three-Dimensional Finite Bodies", ASTM, STP791, 1983.
7. J.C. Newman, Jr. and I.S. Raju, "An Empirical Stress Intensity Factor Equation for the Surface Crack", Journal of Engineering Fracture Mechanics, Vol. 15, pp. 185-192, 1981.
8. G.D. Gupta and F. Erdogan, "The Problem of Edge Cracks in an Infinite Strip", J. Appl. Mech., Vol. 41, pp. 1001-1006, Trans. ASME, 1974.
9. H. Boduroglu and F. Erdogan, "Internal and Edge Cracks in a Plate of Finite Width Under Bending", J. Appl. Mech., Vol. 50, Trans. ASME, pp. 621-629, 1983.
10. E. Reissner, "On Bending of Elastic Plates", Quarterly of Applied Mathematics, Vol. 5, pp. 55-68, 1947-48.
11. F. Delale and F. Erdogan, "Transverse Shear Effect in a Circumferentially Cracked Cylindrical Shell", Quarterly of Applied Mathematics, Vol. 37, pp. 239-258, 1979.
12. A.C. Kaya and F. Erdogan, "Stress Intensity Factors and COD in an Orthotropic Strip", Int. Journal of Fracture, Vol. 16, pp. 171-190, 1980.
13. F. Erdogan, "Mixed Boundary Value Problems in Mechanics", Mechanics-Today, S. Nemat-Nasser, ed. Vol. 4, pp. 1-86, Pergamon Press, Oxford, 1978.
14. J.P. Benthem, "The Quarter Infinite Crack in a Half Space: Alternative and Additional Solutions", Int. J. Solids Structures, Vol. 16, pp. 119-130, 1980.

Appendix A

The definition of normalized quantities

$$x = x_1/a^* , y = x_2/a^* , z = x_3/a^* , \quad (A.1)$$

$$u = u_1/a^* , v = u_2/a^* , w = u_3/a^* , \quad (A.2)$$

$$\phi = \frac{F}{a^{*2}hE} , \beta_x = \beta_1 , \beta_y = \beta_2 , \quad (A.3)$$

$$\sigma_{xx} = \sigma_{11}/E , \sigma_{yy} = \sigma_{22}/E , \sigma_{xy} = \sigma_{12}/E , \quad (A.4)$$

$$N_{\alpha\beta} = \frac{N_{ij}}{hE} , M_{\alpha\beta} = \frac{M_{ij}}{h^2E} , (\alpha,\beta) = (x,y) , (i,j) = (1,2) , \quad (A.5)$$

$$V_x = V_1/hB , V_y = V_2/hB , \quad (A.6)$$

$$B = \frac{5}{6} \frac{E}{2(1+\nu)} , \kappa = \frac{E}{B\lambda^4} , \lambda^4 = 12(1-\nu^2)a^{*2}/h^2 . \quad (A.7)$$

$$b' = b/a^* , c' = c/a^* , d' = d/a^*$$

In the problem described by Fig. 1, $a^* = a = (d-c)/2$ for $0 < c < d \leq b$ and $a^* = d$ for $c = 0, d < b$.

Appendix B

The Fredholm kernels k_1 and k_2 which appear in the integral equations (36) and (37)

$$k_1(x, t) = \int_0^\infty \frac{e^{-(2b'-t)\beta}}{1+4\beta b' e^{-2\beta b'} - e^{-4\beta b'}} \{-[1+(3+2\beta b')e^{-2\beta b'}] \cosh \beta x - 2\beta x e^{-2\beta b'} \sinh \beta x - [2\beta x \sinh \beta x + (3-2\beta b' + e^{-2\beta b'}) \cosh \beta x][1-2\beta(b'-t)]\} d\beta, \quad (B.1)$$

$$k_2(x, t) = \int_0^\infty \left\{ \left[-\frac{3+v}{1+v} - \frac{1-v}{1+v} \beta(b'-t) \right] \frac{1+e^{-2\beta x}}{1-e^{-2\beta b'}} e^{-(2b'-t-x)\beta} - \frac{2\kappa(1-v)}{1+v} \frac{1+e^{-2r_2 x}}{1-e^{-2r_2 b'}} (\beta^2 e^{-(b'-t)r_2} - \beta r_2 e^{-(b'-t)\beta}) e^{-(b'-x)r_2} + \left[\left(\frac{2\beta}{1-v} - \frac{2b'\beta^2}{1+v} \frac{1+e^{-2b'\beta}}{1-e^{-2b'\beta}} \right) (1+e^{-2\beta x}) + \frac{4}{1+v} \{\kappa\beta^3(1+e^{-2\beta x}) + \frac{\beta^2}{2} x(1-e^{-2\beta x}) - \frac{v}{1-v} \beta(1+e^{-2\beta x})\} \right] \frac{1}{D} D_1 e^{-(2b'-t-x)\beta} + D_2 e^{-(b'-x)\beta} e^{-(b'-t)r_2} \right] - \frac{4\kappa}{1+v} \beta^2 r_2 (1+e^{-2r_2 x}) \frac{1}{D} [D_1 e^{-(b'-t)\beta} + D_2 e^{-(b'-t)r_2}] \frac{1-e^{-2b'\beta}}{1-e^{-2b'r_2}} e^{-(b'-x)r_2} \} d\beta, \quad (B.2)$$

$$D_1 = \frac{2\beta}{\gamma^2} r_2 (1-e^{-2b'\beta}) \frac{1+e^{-2b'r_2}}{1-e^{-2b'r_2}} - 2(1+e^{-2b'\beta}) + \frac{1+e^{-2b'\beta}}{\kappa\gamma^2} [1-(b'-t)\beta] - (1-v) \left[\frac{\beta}{2} (b'-t) - \kappa\beta^2 \right] (1-e^{-2b'\beta}), \quad (B.3)$$

$$D_2 = - \frac{2\beta^2}{\gamma^2} \frac{1+e^{-2b'r_2}}{1-e^{-2b'r_2}} (1-e^{-2b'\beta}) - \kappa\beta^2(1-\nu)(1-e^{-2b'\beta}) , \quad (B.4)$$

$$D = 4b'\beta^2 e^{-2b'\beta} - \left(\frac{3+\nu}{1-\nu}\beta + 2\kappa\beta^3\right)(1-e^{-4b'\beta}) \\ + 2\beta^2\kappa r_2 \frac{1+e^{-2b'r_2}}{1-e^{-2b'r_2}} (1-e^{-2b'\beta})^2 . \quad (B.5)$$

Table 1. The normalized stress intensity factors at the maximum penetration point ($x=0$) of a symmetrically located single semi-elliptic surface crack in a plate under uniform tension or bending ($\nu=0.3$).

$\frac{b}{h}$	$\frac{d}{h}$	$L_o = 0.2h$		$L_o = 0.4h$		$L_o = 0.6h$		$L_o = 0.8h$	
		$k_b(0)$	$k_t(0)$	$k_b(0)$	$k_t(0)$	$k_b(0)$	$k_t(0)$	$k_b(0)$	$k_t(0)$
10	0.5	.709	.729	.308	.390	.0518	.175	-.0290	0.0503
	0.6	.737	.755	.342	.421	.0705	.192	-.0257	.0555
	0.8	.777	.792	.398	.470	.104	.221	-.0188	.0648
	1	.805	.818	.443	.508	.132	.246	-.0121	.0730
	4/3	.837	.848	.501	.559	.174	.282	-.0014	.0848
	2	.876	.884	.584	.630				
	4	.930	.934	.723	.752	.390	.464	.0726	.155
	6	.953	.956	.800	.819	.499	.556	.127	.203
	8	.967	.969	.853	.865	.592	.634	.190	.256
	9.5	.975	.976	.885	.893	.659	.689	.249	.305
	9.61	.976	.977	.887	.894	.664	.693	.254	.310
	9.8	.977	.978	.891	.898	.672	.700	.264	.318
8	0.5	.709	.729	.308	.390	.0519	.175	-.0290	.0503
	0.6	.738	.755	.342	.421	.0706	.192	-.0256	.0556
	0.8	.778	.792	.399	.470	.104	.221	-.0188	.0649
	1	.805	.818	.444	.509	.133	.247	-.0120	.0731
	2	.877	.885	.586	.632	.246	.341	.0189	.105
	4	.932	.936	.730	.758	.400	.472	.0774	.159
	6	.957	.959	.814	.830	.525	.576	.144	.216
	7.69	.971	.972	.867	.876	.626	.660	.223	.282
	7.84	.972	.973	.872	.880	.635	.667	.233	.290
6	0.5	.710	.729	.307	.391	.0521	.176	-.0289	.0503
	0.6	.738	.756	.343	.422	.0710	.192	-.0256	.0556
	0.9	.794	.807	.424	.492	.122	.235	-.0152	.0693
	1.2	.827	.839	.483	.543	.160	.270	-.0051	.0807
	1.5	.851	.861	.530	.583	.196	.301	.0046	.0910
	3	.915	.920	.681	.715	.341	.423	.0531	.137
	4	.930	.934	.723	.752	.390	.464	.0726	.155
	5	.953	.955	.802	.818	.507	.560	.136	.208
	5.77	.963	.964	.839	.850	.576	.616	.187	.250
	5.88	.964	.965	.844	.855	.587	.625	.197	.258

Table 1 (cont)

$\frac{b}{h}$	$\frac{d}{h}$	$L_o = 0.2h$		$L_o = 0.4h$		$L_o = 0.6h$		$L_o = 0.8h$	
		$k_b(0)$	$k_t(0)$	$k_b(0)$	$k_t(0)$	$k_b(0)$	$k_t(0)$	$k_b(0)$	$k_t(0)$
4	0.5	.711	.730	.309	.392	.0528	.176	-.0289	.0504
	0.666	.755	.771	.366	.441	.0839	.204	-.0231	.0591
	0.8	.780	.795	.403	.474	.106	.223	-.0184	.0653
	1	.809	.821	.450	.514	.137	.250	-.0112	.0738
	1.33	.843	.853	.512	.568	.183	.289	.0006	.0866
	1.5	.856	.865	.540	.591	.204	.307	.0068	.0929
	2	.886	.893	.608	.650	.265	.358	.0257	.111
	3.92	.951	.953	.800	.815	.519	.565	.152	.218
2	0.5	.716	.735	.316	.398	.0557	.179	-.0287	.0508
	0.6	.747	.763	.355	.431	.0768	.197	-.0249	.0564
	0.8	.791	.804	.421	.488	.117	.232	-.0166	.0671
	0.9	.808	.820	.450	.513	.136	.248	-.0121	.0722
	1.0	.823	.843	.477	.537	.156	.265	-.0072	.0774
	4/3	.864	.872	.561	.608	.224	.321	.0118	.0961
	1.9	.916	.919	.701	.726	.385	.450	.0754	.150
	1.96	.920	.924	.718	.740	.411	.471	.0903	.162

Table 2. Distribution of the stress intensity factors along the crack front in a plate containing a single symmetric semi-elliptic surface crack ($b/h = 10$, $\nu = 0.3$, $x = x_1/d$).

	k_b	k_t	k_b	k_t	k_b	k_t	k_b	k_t
L_o/h	0.2		0.4		0.6		0.8	
x	$b/h = 10, d/h = 0.5, \nu = 0.3$							
0.929	0.628	.547	.428	.340	.191	.152	.0486	.444
0.828	.672	.609	.392	.349	.154	.156	.0314	.472
0.688	.694	.656	.361	.364	.123	.162	.0113	.510
0.516	.704	.691	.336	.376	.0924	.169	-.0061	.512
0.319	.708	.715	.318	.385	.0672	.173	-.0187	.502
0.108	.709	.727	.308	.390	.0535	.175	-.0276	.503
0	.709	.729	.307	.390	.0518	.175	-.0290	.503

$b/h = 10, d/h = 1, \nu = 0.3$								
0.929	.631	.545	.505	.391	.272	.205	.0809	.0649
0.828	.709	.639	.496	.426	.239	.215	.0621	.0677
0.688	.756	.710	.480	.457	.209	.226	.0396	.0718
0.516	.783	.762	.464	.482	.177	.236	.0183	.0729
0.319	.798	.798	.451	.499	.149	.243	.0163	.0724
0.108	.804	.816	.444	.507	.134	.246	-.0103	.0728
0	.805	.818	.443	.508	.132	.246	-.0121	.0730

$b/h = 10, d/h = 4, \nu = 0.3$								
0.929	.623	.535	.561	.420	.402	.285	.168	.121
0.828	.739	.661	.626	.517	.420	.339	.163	.137
0.688	.819	.763	.666	.601	.426	.387	.144	.150
0.516	.875	.844	.695	.671	.418	.425	.120	.156
0.319	.910	.901	.713	.722	.402	.451	.0953	.156
0.108	.927	.930	.722	.748	.391	.463	.0756	.155
0	.930	.934	.723	.752	.390	.464	.0726	.155

$b/h = 10, d/h = 8, \nu = 0.3$								
0.929	.622	.533	.571	.423	.453	.316	.238	.170
0.828	.747	.667	.665	.542	.513	.403	.260	.209
0.688	.837	.778	.735	.653	.560	.487	.261	.240
0.516	.901	.868	.791	.749	.586	.558	.245	.256
0.319	.944	.931	.830	.821	.593	.607	.219	.259
0.108	.965	.965	.850	.860	.592	.631	.194	.256
0	.967	.969	.853	.865	.592	.634	.190	.256

Table 2 (cont.)

	k_b	k_t	k_b	k_t	k_b	k_t	k_b	k_t
L_o/h	0.2		0.4		0.6		0.8	
x	$b/h = 10 \text{ , } d/h = 9.8 \text{ , } \nu = 0.3$							
0.929	.629	.538	.597	.442	.508	.355	.312	.225
0.828	.753	.673	.692	.562	.572	.446	.341	.270
0.688	.844	.784	.763	.675	.626	.536	.345	.305
0.516	.909	.875	.822	.775	.658	.614	.328	.323
0.319	.952	.939	.865	.851	.670	.669	.298	.324
0.108	.974	.973	.888	.892	.672	.697	.268	.319
0	.977	.978	.891	.898	.672	.700	.264	.318

Table 3. Distribution of the stress intensity factors along the crack front in a plate containing a single symmetric semi-elliptic surface crack ($b/h = 2, 4, 6$; $\nu = 0.3$).

	k_b	k_t	k_b	k_t	k_b	k_t	k_b	k_t
L_o/h	0.2		0.4		0.6		0.8	
x	$b/h = 2, d/h = 1, \nu = 0.3$							
0.929	.646	.559	.542	.421	.306	.232	.0941	0.0752
0.828	.726	.654	.533	.456	.271	.240	.0736	.0768
0.688	.774	.726	.517	.487	.238	.249	.0492	.0796
0.516	.801	.779	.500	.511	.204	.257	.0261	.0793
0.319	.816	.814	.486	.527	.174	.262	.0077	.0777
0.108	.823	.832	.478	.536	.158	.264	-.0053	.0774
0	.823	.834	.477	.537	.156	.265	-.0072	.0774
$b/h = 4, d/h = 1, \nu = 0.3$								
0.929	.634	.548	.512	.397	.278	.210	.0833	.0668
0.828	.713	.642	.504	.432	.245	.220	.0642	.0694
0.688	.760	.713	.488	.463	.214	.230	.0414	.0733
0.516	.787	.766	.471	.488	.182	.240	.0198	.0741
0.319	.802	.801	.458	.505	.154	.246	.0028	.0734
0.108	.808	.819	.451	.513	.139	.249	-.0094	.0737
0	.809	.821	.450	.514	.137	.250	-.0112	.0738
$b/h = 6, d/h = 1.2, \nu = 0.3$								
0.929	.632	.545	.522	.402	.296	.221	.0921	.0723
0.828	.717	.645	.523	.446	.266	.234	.0732	.0754
0.688	.770	.722	.513	.483	.237	.247	.0501	.0796
0.516	.801	.778	.501	.512	.206	.258	.0277	.0808
0.319	.819	.817	.490	.532	.178	.266	.0096	.0802
0.108	.827	.836	.474	.541	.162	.270	-.0032	.0806
0	.827	.839	.483	.543	.160	.270	-.0051	.0807

Table 4. The normalized stress intensity factors at the center ($x=0$) of a single symmetric rectangular surface crack in a plate under tension or bending ($\nu=0.3$).

$\frac{b}{h}$	$\frac{d}{h}$	$L_o = 0.2h$		$L_o = 0.4h$		$L_o = 0.6h$		$L_o = 0.8h$	
		$k_b(0)$	$k_t(0)$	$k_b(0)$	$k_t(0)$	$k_b(0)$	$k_t(0)$	$k_b(0)$	$k_t(0)$
10	0.5	.765	.784	.340	.429	.0607	.194	-.0316	.0599
	2	.915	.922	.652	.699	.284	.388	.0261	.122
	5	.970	.973	.847	.868	.544	.611	.134	.222
	9.8	.999	.999	.987	.989	.914	.927	.557	.603
8	0.5	.766	.785	.340	.429	.0608	.194	-.0316	.0599
	1	.853	.865	.496	.563	.154	.276	-.0105	.0851
	4	.963	.966	.814	.840	.487	.562	.104	.195
	7.84	.998	.998	.982	.985	.892	.907	.503	.554
6	0.5	.766	.785	.341	.429	0.0610	.194	-.0316	.0600
	1	.855	.867	.498	.566	.155	.277	-.0103	.0854
	3	.951	.955	.767	.797	.414	.500	.0721	.165
	5.88	.997	.998	.975	.978	.857	.878	.434	.491
4	0.5	.768	.787	.343	.431	0.0619	.195	-.0315	.0602
	1	.859	.870	.505	.571	.159	.281	-.0095	.0863
	2	.930	.936	.690	.732	.320	.419	.0370	.133
	3.92	.996	.996	.959	.965	.797	.826	.341	.408
2	0.5	.776	.794	.352	.439	.0655	.198	-.0312	.0609
	1	.880	.890	.545	.606	.186	.304	-.0041	.0923
	1.5	.941	.945	.710	.749	.334	.432	.0395	.135
	1.96	.990	.991	.916	.927	.666	.715	.205	.285

Table 5. Distribution of the stress intensity factors along the crack front in a plate containing a single symmetric rectangular surface crack, $x = x_1/d$.

	k_b	k_t	k_b	k_t	k_b	k_t	k_b	k_t
L_o/h	0.2		0.4		0.6		0.8	
x	$b/h = 2, d/h = 1, \nu = 0.3$							
0.929	.585	.618	.233	.334	.0289	.159	-.0295	0.0458
0.828	.737	.759	.354	.440	.0798	.209	-.0261	.0619
0.688	.814	.829	.439	.514	.122	.248	-.0190	.0741
0.516	.852	.864	.495	.562	.154	.276	-.0120	.0831
0.319	.871	.881	.528	.591	.174	.294	-.0070	.0890
0.108	.879	.889	.543	.605	.184	.302	-.0044	.0920
0	.880	.890	.545	.606	.186	.304	-.0041	.0923
$b/h = 6, d/h = 1, \nu = 0.3$								
0.929	.566	.601	.210	.314	.0181	.149	-.0302	.0439
0.828	.715	.738	.321	.411	.0623	.194	-.0283	.0586
0.688	.789	.806	.399	.480	.0996	.228	-.0227	.0694
0.516	.827	.841	.451	.524	.127	.253	-.0169	.0773
0.319	.846	.858	.482	.551	.145	.269	-.0127	.0825
0.108	.854	.866	.496	.564	.154	.276	-.0105	.0851
0	.855	.867	.498	.566	.155	.277	-.0103	.0854
$b/h = 10, d/h = 1, \nu = 0.3$								
0.929	.423	.470	.112	.228	-.0172	.108	-.0293	.0309
0.828	.574	.609	.191	.298	.0038	.138	-.0343	.0417
0.688	.667	.694	.252	.352	.0250	.160	-.0350	.0492
0.516	.721	.744	.297	.390	.0421	.177	-.0339	.0545
0.319	.751	.771	.325	.415	.0539	.188	-.0325	.0580
0.108	.764	.783	.339	.427	.0599	.193	-.0317	.0597
0	.765	.784	.340	.429	.0607	.194	-.0316	.0599

Table 6. The location $x=x^*$ and magnitude $k_b(x^*)$ and $k_t(x^*)$ of the normalized stress intensity factors in a plate containing two collinear semi-elliptic surface cracks, $D=a/(a+c)$.

D		$L_o = 0.2h$		$L_o = 0.4h$		$L_o = 0.6h$		$L_o = 0.8h$	
		$k_b(x^*)$	$k_t(x^*)$	$k_b(x^*)$	$k_t(x^*)$	$k_b(x^*)$	$k_t(x^*)$	$k_b(x^*)$	$k_t(x^*)$
0.112	x^*	0.2	0.05	.929	.319	.929	.929	.929	.929
	$k(x^*)$.831	.839	.649	.554	.409	.308	.138	.107
0.125	x^*	0	0	.929	.040	.929	.108	.929	.516
	$k(x^*)$.812	.824	.522	.518	.287	.523	.867	.756
.250	x^*	0	0	$\bar{+}$.929	0	.929	0	.929	$\bar{+}$.516
	$k(x^*)$.807	.820	.509	.512	.275	.248	.0822	.735
0.5	x^*	0	0	-.929	0	-.929	0	-.828	.516
	$k(x^*)$.811	.823	.521	.517	.285	.251	.0858	.0744
0.75	x^*	-0.50	0	-.929	-.050	-.929	-.108	-.929	-.688
	$k(x^*)$.818	.829	.550	.528	.310	.259	.0951	.786

Table 7. Distribution of the normalized stress intensity factors along the crack front in a plate containing two collinear semi-elliptic surface cracks, $\bar{x} = [x_1 - (c+a)]/a$ (Fig. 1).

	k_b	k_t	k_b	k_t	k_b	k_t	k_b	k_t
L_o/h	0.2		0.4		0.6		0.8	
\bar{x}	$b/h = 10, d/h = 1, D = a/(c+a)=0.112, \nu=0.3$							
0.929	.688	.596	.649	.505	.409	.308	.138	.107
0.828	.766	.689	.623	.527	.351	.300	.106	.102
0.688	.805	.754	.584	.541	.297	.294	.0720	.0975
0.516	.824	.798	.548	.550	.246	.289	.0411	.0915
0.319	.831	.827	.519	.554	.204	.285	.0175	.0858
0.108	.831	.839	.500	.553	.178	.280	.0013	.0829
0	.829	.839	.494	.550	.173	.278	-.0016	.0821
-0.108	.826	.835	.491	.546	.172	.275	-.0004	.0814
-0.319	.816	.814	.492	.532	.184	.269	.0117	.0809
-0.516	.799	.776	.500	.512	.209	.261	.0293	.0818
-0.688	.769	.721	.513	.484	.240	.250	.0516	.0814
-0.828	.720	.649	.526	.450	.270	.239	.0751	.0780
-0.929	.640	.553	.533	.413	.303	.229	.0949	.0758
$b/h = 10, d/h = 1, D = a/(c+a)=0.75, \nu = 0.3$								
0.929	.637	.551	.521	.404	.288	.217	.0872	.0698
0.828	.716	.645	.514	.440	.254	.227	.0678	.0721
0.688	.764	.717	.499	.472	.224	.237	.0446	.0757
0.516	.793	.771	.484	.498	.192	.247	.0225	.0763
0.319	.809	.807	.472	.516	.164	.254	.0050	.0753
0.108	.816	.826	.467	.526	.149	.258	-.0075	.0754
0	.818	.829	.467	.528	.148	.258	-.0093	.0755
-0.108	.818	.828	.469	.528	.151	.259	-.0073	.0755
-0.319	.814	.812	.480	.522	.169	.258	.0057	.0760
-0.516	.801	.778	.497	.509	.200	.253	.0243	.0778
-0.688	.776	.727	.517	.488	.236	.247	.0481	.0786
-0.828	.730	.657	.538	.460	.272	.240	.0735	.0766
-0.929	.651	.563	.550	.427	.310	.235	.0951	.0757

Table 8. The normalized intensity factors on the edges ($x=\pm b'$) of a plate containing two symmetric corner cracks having a profile of a quarter ellipse (Fig. 1).

$\frac{b}{h}$	$\frac{a}{h}$	$L_o = 0.2h$		$L_o = 0.4h$		$L_o = 0.6h$		$L_o = 0.8h$	
		$k_b(b')$	$k_t(b')$	$k_b(b')$	$k_t(b')$	$k_b(b')$	$k_t(b')$	$k_b(b')$	$k_t(b')$
2	0.25	.775	.790	.380	.485	.0975	.219	-.0172	.0678
	0.3	.797	.810	.415	.485	.120	.239	-.0117	.0743
	0.4	.828	.840	.473	.535	.159	.271	-.0014	.0857
	0.5	.852	.862	.522	.477	.197	.303	.0089	.0963
	0.6	.872	.880	.568	.616	.234	.334	.0199	.107
	0.7	.889	.896	.610	.652	.273	.366	.0321	.118
	0.8	.905	.910	.653	.688	.317	.401	.0470	.131
4	0.26	.777	.792	.384	.459	.102	.223	-.0152	.0700
	0.4	.821	.833	.463	.527	.156	.269	.0003	.0873
	0.6	.858	.867	.539	.593	.215	.319	.0179	.106
	0.8	.883	.890	.597	.642	.264	.361	.0336	.121
	1	.901	.907	.644	.683	.310	.399	.0492	.136
	1.2	.916	.921	.685	.718	.354	.435	.0657	.150
	1.4	.929	.933	.722	.750	.398	.471	.0838	.166
	1.6	.939	.942	.756	.779	.443	.508	.105	.184
6	0.27	.781	.796	.391	.464	.106	.226	-.0140	.0714
	0.3	.792	.806	.410	.481	.119	.237	-.0105	.0755
	0.6	.856	.866	.536	.591	.214	.319	.0187	.107
	0.9	.889	.896	.613	.657	.281	.376	.0409	.128
	1.2	.910	.916	.669	.705	.337	.422	.0609	.147
	1.5	.926	.930	.713	.744	.387	.464	.0809	.165
	1.8	.938	.941	.750	.776	.434	.503	.102	.183
	2.1	.948	.950	.782	.803	.479	.540	.124	.202
	2.4	.956	.958	.811	.828	.523	.576	.149	.223
8	.28	.785	.799	.397	.470	.110	.230	-.0129	.0727
	0.4	.821	.833	.462	.526	.156	.269	.0004	.0875
	0.8	.879	.887	.589	.636	.260	.358	.0343	.122
	1.2	.908	.914	.665	.702	.334	.420	.0607	.147
	1.6	.927	.932	.718	.748	.394	.470	.0846	.168
	2	.941	.944	.760	.784	.447	.514	.108	.189
	2.4	.951	.953	.793	.813	.494	.554	.133	.210
	2.8	.959	.961	.821	.837	.538	.591	.158	.232
	3.2	.965	.967	.845	.858	.580	.626	.186	.255

Table 8 - cont.

$\frac{b}{h}$	$\frac{a}{h}$	$L_o = 0.2h$		$L_o = 0.4h$		$L_o = 0.6h$		$L_o = 0.8h$	
		$k_b(b')$	$k_t(b')$	$k_b(b')$	$k_t(b')$	$k_b(b')$	$k_t(b')$	$k_b(b')$	$k_t(b')$
10	0.25	.772	.787	.376	.452	.0967	.218	-.0165	.0684
	0.75	.873	.882	.576	.625	.249	.349	.0307	.118
	1	.895	.902	.630	.672	.299	.391	.0483	.135
	1.5	.922	.927	.704	.736	.378	.457	.0786	.163
	2	.939	.943	.755	.780	.440	.510	.106	.188
	2.5	.951	.953	.793	.813	.494	.555	.133	.211
	3.0	.959	.961	.823	.840	.541	.594	.160	.234
	3.5	.966	.968	.848	.861	.584	.630	.188	.258
	4.0	.972	.973	.869	.880	.624	.664	.218	.283
	4.5	.976	.977	.888	.896	.664	.696	.252	.312
20	1	.895	.901	.629	.671	.298	.390	.0483	.135

Table 9. Distribution of the normalized stress intensity factors along the crack front in a plate containing two (elliptic) corner cracks, $\bar{x} = [x_1 - (c+a)]/a$ (Fig. 1).

	k_b	k_t	k_b	k_t	k_b	k_t	k_b	k_t
L_o/h	0.2		0.4		0.6		0.8	
\bar{x}	$b/h = 2, a/h = 0.5, \nu = 0.3$							
0.999	.852	.862	.522	.577	.197	.303	.0089	.0963
0.936	.846	.856	.515	.571	.191	.297	.0073	.0936
0.784	.834	.843	.503	.557	.182	.286	.0050	.0883
0.558	.824	.828	.493	.543	.177	.274	.0064	.0834
0.279	.813	.808	.492	.528	.184	.266	.0138	.0805
-0.026	.799	.777	.498	.510	.204	.257	.0263	.0798
-0.329	.776	.732	.511	.488	.231	.248	.0450	.0794
-0.600	.736	.669	.526	.460	.261	.240	.0679	.0768
-0.815	.668	.583	.537	.427	.294	.231	.0882	.0748
-0.953	.549	.460	.532	.390	.336	.232	.112	.0772

$b/h = 8, a/h = 0.8, \nu = 0.3$								
0.999	.879	.887	.589	.636	.260	.358	.0343	.122
0.936	.874	.882	.582	.630	.253	.351	.0317	.118
0.784	.866	.872	.570	.617	.242	.339	.0277	.112
0.558	.857	.859	.561	.602	.237	.326	.0281	.105
0.279	.844	.836	.557	.583	.243	.314	.0357	.101
-0.026	.825	.800	.557	.559	.259	.302	.0489	.0990
-0.329	.793	.746	.558	.525	.282	.286	.0677	.0966
-0.600	.741	.671	.558	.481	.304	.269	.0896	.0917
-0.815	.658	.573	.547	.428	.326	.249	.108	.0869
-0.953	.521	.434	.502	.361	.345	.231	.127	.0850

Table 10. The normalized stress intensity factors at the edges $x = \pm b'$ of a plate containing two symmetric rectangular corner cracks.

$\frac{b}{h}$	$\frac{a}{h}$	$L_o = 0.2h$		$L_o = 0.4h$		$L_o = 0.6h$		$L_o = 0.8h$	
		$k_b(b')$	$k_t(b')$	$k_b(b')$	$k_t(b')$	$k_b(b')$	$k_t(b')$	$k_b(b')$	$k_t(b')$
2	0.25	.821	.835	.415	.494	.108	.238	-.0185	.0773
	0.5	.895	.903	.581	.638	.223	.337	-.0119	.109
	0.8	.954	.958	.754	.787	.388	.477	.0620	.156
4	0.26	.820	.835	.419	.497	.112	.242	-.0163	.0797
	0.4	.860	.871	.507	.574	.174	.295	.0014	.0985
	1	.937	.942	.716	.755	.359	.453	.0595	.154
	1.6	.976	.978	.856	.876	.550	.617	.139	.227
6	0.27	.823	.838	.426	.504	.117	.246	-.0149	0.0812
	0.6	.891	.900	.589	.645	.240	.353	.0227	.120
	1.6	.956	.960	.788	.817	.453	.534	.0983	.190
	2.4	.984	.985	.902	.915	.648	.700	.202	.283
8	0.28	.827	.841	.433	.510	.122	.250	-.0136	.0826
	0.8	.912	.919	.648	.696	.294	.399	.0409	.138
	2	.967	.970	.833	.856	.525	.595	.133	.222
	3.2	.988	.989	.927	.937	.714	.756	.255	.331
10	0.27	.823	.837	.425	.503	.117	.246	-.0150	.0811
	1	.927	.933	.692	.734	.341	.439	.0573	.153
	2.5	.974	.976	.864	.882	.581	.643	.165	.251
	4	.991	.992	.943	.951	.761	.796	.302	.374

Table 11. Distribution of the normalized stress intensity factors in a plate with rectangular corner cracks, $\bar{x} = [x_1 - (c+a)]/a$.

	k_b	k_t	k_b	k_t	k_b	k_t	k_b	k_t
L_o/h	0.2		0.4		0.6		0.8	
\bar{x}	$b/h = 2, a/h = 0.5, \nu = 0.3$							
0.999	.895	.903	.581	.638	.223	.337	.0119	.109
0.936	.892	.901	.576	.634	.218	.332	.0102	.107
0.784	.887	.896	.564	.623	.207	.323	.0059	.103
0.558	.879	.889	.548	.609	.193	.310	.0003	.0967
0.279	.868	.879	.525	.589	.175	.295	-.0057	.0902
-0.026	.851	.863	.493	.561	.153	.275	-.0122	.0828
-0.329	.818	.833	.444	.518	.124	.249	-.0195	.0739
-0.600	.756	.776	.370	.454	.0852	.214	-.0268	.0626
-0.815	.630	.660	.262	.359	.0373	.168	-.0314	.0481
-0.953	.385	.434	.115	.229	-.0098	.107	-.0260	.0284
$b/h = 8, a/h = 0.8, \nu = 0.3$								
0.999	.912	.919	.648	.696	.294	.399	.0409	.138
0.936	.911	.918	.643	.692	.289	.394	.0383	.135
0.784	.907	.915	.633	.683	.277	.384	.0322	.129
0.558	.902	.910	.619	.671	.261	.370	.0249	.121
0.279	.894	.902	.598	.652	.242	.353	.0172	.114
-0.026	.880	.890	.567	.625	.217	.331	.0086	.105
-0.329	.856	.868	.520	.584	.183	.301	-.0015	.0934
-0.600	.809	.824	.446	.520	.137	.260	-.0133	.0792
-0.815	.705	.729	.331	.420	.0759	.205	-.0245	.0610
-0.953	.462	.505	.160	.270	.0073	.131	-.0263	.0367

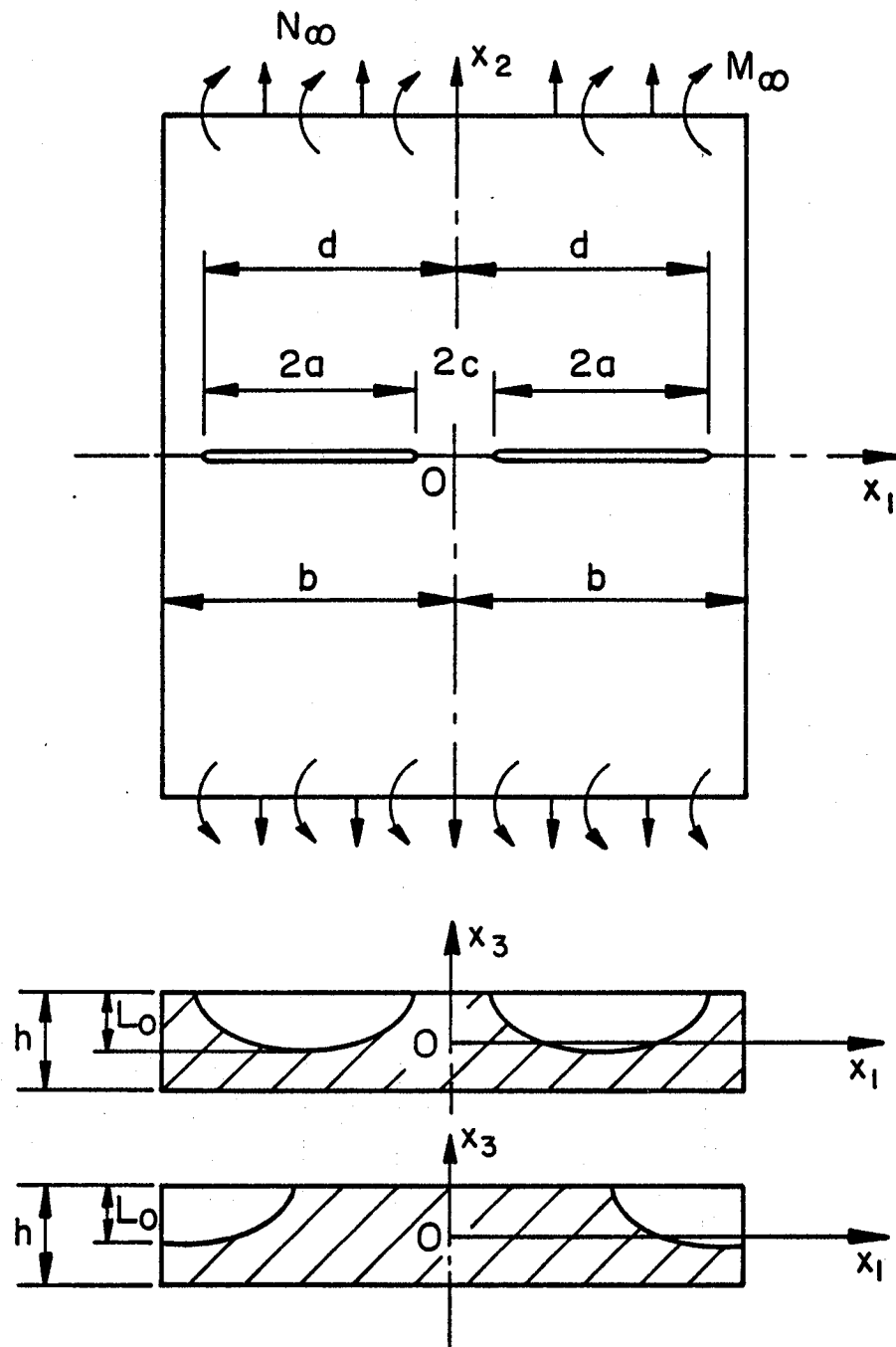


Fig. 1 The geometry of the plate with surface cracks

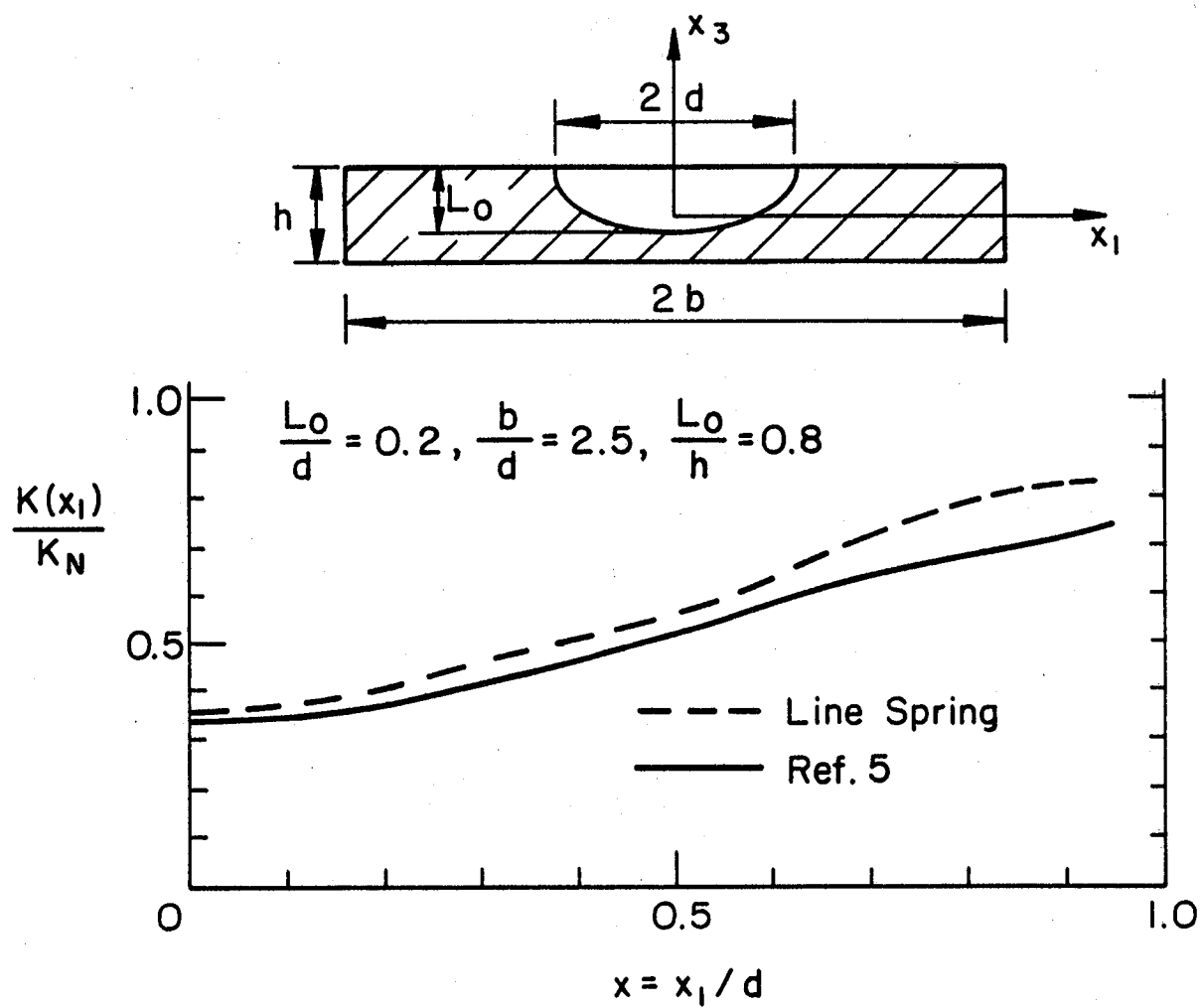


Fig. 2 Comparison of stress intensity factors calculated by the finite element and line spring methods in a plate containing a symmetrically located semi-elliptic surface crack and subjected to uniform tension.

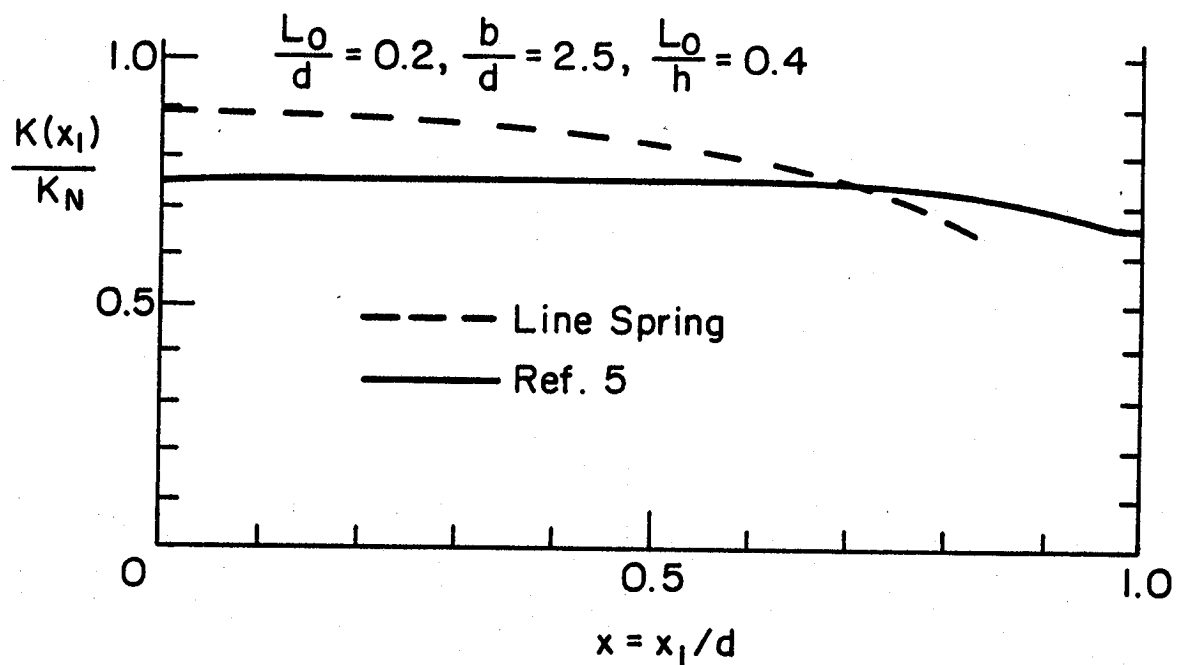
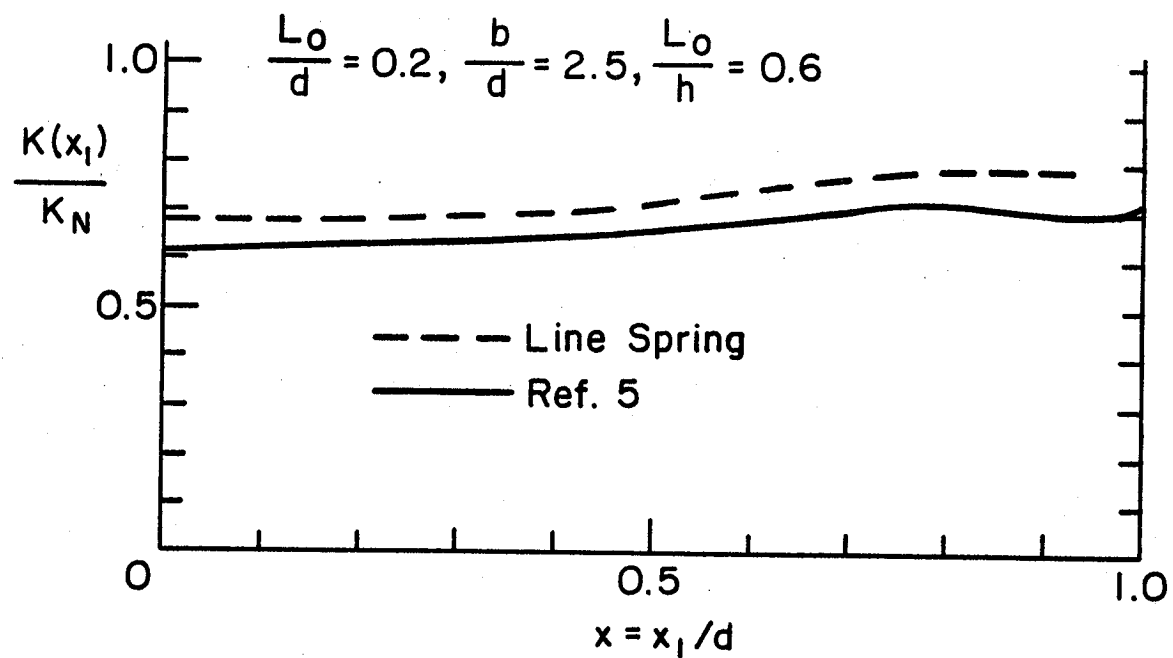


Fig. 3 Comparison of the stress intensity factors calculated by the finite element and line spring methods in a plate containing a single symmetric semi-elliptic surface crack and subjected to uniform bending.

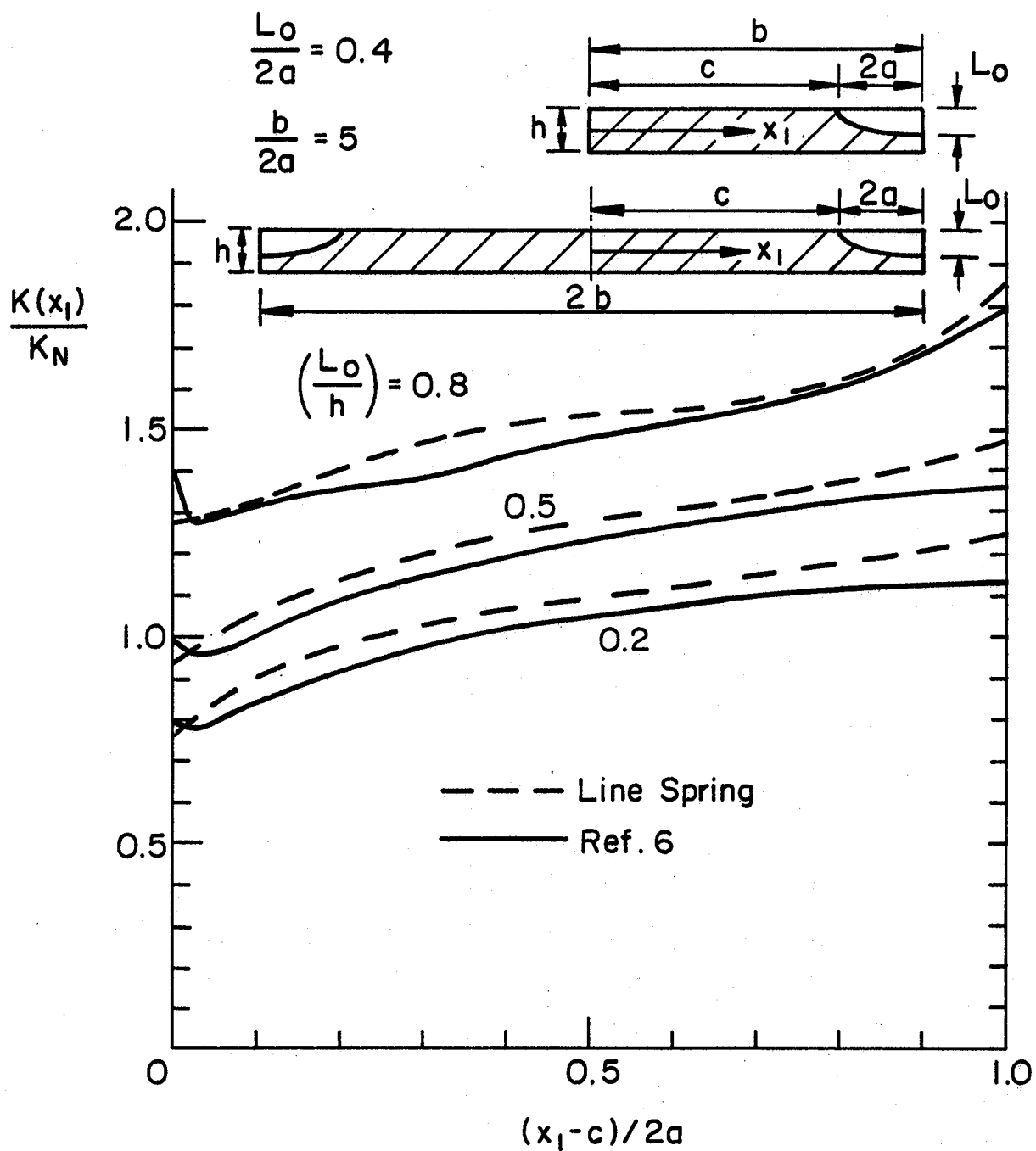


Fig. 4 Comparison of the stress intensity factors calculated by the finite element and line spring methods in a plate containing elliptic corner cracks and subjected to uniform tension, $L_0/2a = 0.4$, $b/2a = 5$.

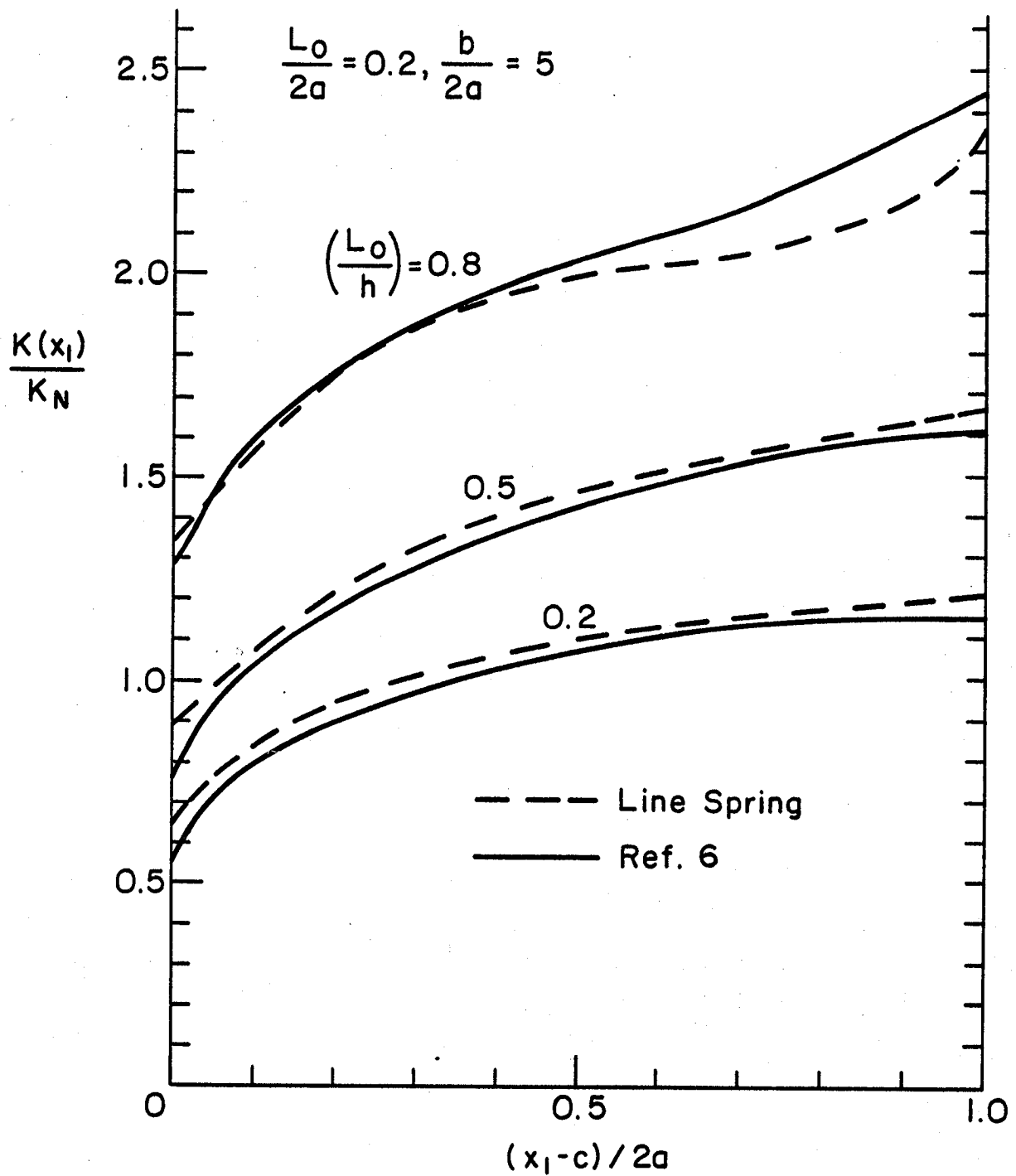


Fig. 5 Comparison of the stress intensity factors calculated by the finite element and line spring methods in a plate containing elliptic corner cracks and subjected to uniform tension, $L_o/2a = 0.2$, $b/2a = 5$.

1. Report No. NASA CR- 172309		2. Government Accession No.		3. Recipient's Catalog No.	
4. Title and Subtitle SURFACE CRACKS IN A PLATE OF FINITE WIDTH UNDER EXTENSION OR BENDING				5. Report Date February 1984	
				6. Performing Organization Code	
7. Author(s) F. Erdogan and H. Boduroglu				8. Performing Organization Report No.	
9. Performing Organization Name and Address Lehigh University Bethlehem, PA 18015				10. Work Unit No.	
				11. Contract or Grant No. NGR-39-007-011	
				13. Type of Report and Period Covered Contractor Report	
12. Sponsoring Agency Name and Address National Aeronautics and Space Administration Washington, DC 20546				14. Sponsoring Agency Code	
15. Supplementary Notes Langley technical monitor: W. S. Johnson					
16. Abstract In this paper the problem of a finite plate containing collinear surface cracks is considered. The problem is solved by using the line spring model with plane elasticity and Reissner's plate theory. The main purpose of the study is to investigate the effect of interaction between two cracks or between cracks and stress-free plate boundaries on the stress intensity factors and to provide extensive numerical results which may be useful in applications. First, some sample results are obtained and are compared with the existing finite element results. Then the problem is solved for a single (internal) crack, two collinear cracks, and two corner cracks for wide range of relative dimensions. Particularly in corner cracks the agreement with the finite element solution is surprisingly very good. The results are obtained for semi-elliptic and rectangular crack profiles which may, in practice, correspond to two limiting cases of the actual profile of a subcritically growing surface crack.					
17. Key Words (Suggested by Author(s)) Surface cracks Stress intensity factors Line spring model Reissner plate theory			18. Distribution Statement Unclassified - Unlimited Subject Category 39		
19. Security Classif. (of this report) Unclassified	20. Security Classif. (of this page) Unclassified	21. No. of Pages 40	22. Price A03		

